COMMUNICATION

Understanding the abundance of the rare sugar β-D-allose

G. Juarez,[a] E. R. Alonso,[a] M. Sanz-Novo,[a] J. L Alonso,[a] and I. León*[a]

Received 00th January 20xx,
Accepted 00th January 20xx

DOI: 10.1039/x0xx00000x

The conformational landscape of β-D-allose, a rare sugar, has been investigated using laser ablation in combination with high-resolution rotational spectroscopy. Altogether, three species are identified, exhibiting a counter-clockwise intramolecular hydrogen bond network. The effect of epimerization on the main aldohexose is also studied and, despite the main conformers being very similar, the position of the hydroxyl groups in allose allows for the formation of considerably stronger intramolecular hydrogen bonds than in glucose: this could explain the low abundance of β-D-allose in nature.

Carbohydrates are an important class of biomolecules that perform numerous roles in living organisms.[1] For example, they serve for the storage of energy and energy management, and play a key role as structural components.[2] The building blocks of carbohydrates are the monosaccharides, the simplest sugar form. There are more than 50 types of monosaccharides on Earth, each one with characteristic and extraordinary properties.[3,4] Among them, glucose is an aldohexose that deserves a special mention due to being the most abundant monosaccharide, playing a pivotal role in many processes essential to life,[5,6] such as in the energy metabolism of many living organisms[1]. Along with glucose, galactose and mannose are the three aldohexoses that commonly occur naturally. On the other side of the monosaccharide spectrum, other aldohexoses are scarce and known as 'rare sugars',[7] with D-allose being one of the most representative one. It is the C_3 epimer of glucose and has been isolated from the leaves of the Rubropyl Protea, an African bush.[8] Curiously, D-allose is perceived with an intensely sweet taste similar to glucose.[9,10]

Two chiral isomers of glucose and allose are possible, of which only D-glucose and D-allose occur naturally.[11] As shown in Figure 1, D-allose only differs from the archetypal D-glucose in the hydroxyl group at the C_3 position. An X-ray diffraction study[12] shows that crystalline D-allose exists only in the β-pyranose form (Figure 1a) with a $^4C_1$ chair configuration where the hydroxymethyl group is at the energetically favoured equatorial position. Surprisingly, while our body metabolizes D-glucose, D-allose does not, making it a good candidate as an ultra-low calorie sweetener.[9,10] Furthermore, while cellulose, an unbranched polymer of β-D-glucose, is among the most abundant organic compounds in the biosphere,[13] β-D-allose rarely exists in nature. The comparison between D-glucose and D-allose is therefore very interesting, as the variation in the position of a single OH group (see Figure 1) results, not only in molecules with different biological properties, but also in their natural abundance.

Properties of biomolecules are tightly related to their structure. A mandatory step is thus the three-dimensional determination of their structure at a molecular scale.[14] To date, the structure of D-allose has solely been investigated in the condensed phase,[12,15–18] and there is no precise information about the intrinsic structures of D-allose. A powerful method to shed some light on such questions is to study the species free from external perturbation, using an experimental technique that allows structural characterization. Rotational spectroscopy is ideal in this mean. It is one of the most accurate spectroscopic techniques to determine the structure of molecules, which, under supersonic expansions, can be used to unequivocally identify the conformations of the molecule without any interference with the environment.[19,20] Combined with laser ablation, it allows for overcoming the thermolability of biomolecules.[14,21] Altogether, it enables the

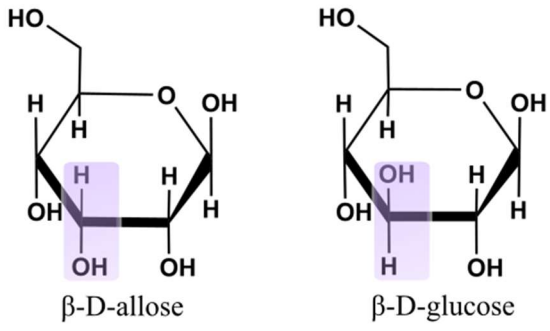

Fig. 1 Chemical structures of β-D-allose and β-D-glucose.

[a] *Grupo de Espectrocopía Molecular (GEM), Edificio Quifima, Laboratorios de Espectroscopia y Bioespectroscopia, Unidad Asociada CSIC, Parque Científico UVa, Universidad de Valladolid, 47011, Valladolid, Spain. E-mail: iker.leon@uva.es*

Electronic Supplementary Information (ESI) available. See DOI: 10.1039/x0xx00000x

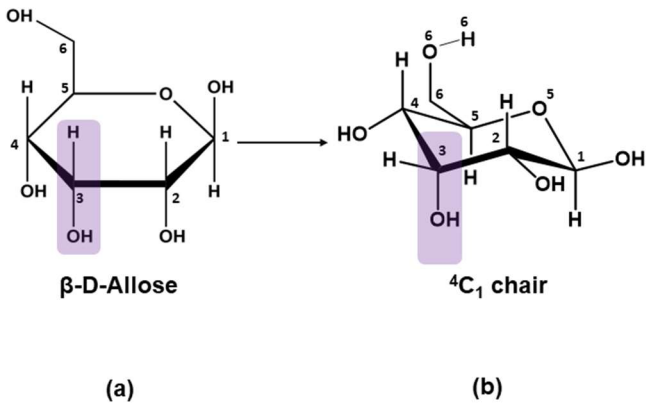

Fig. 2 (a) Haworth projection of β-D-allose. (b) $^4C_1$ chair conformation.

investigations of the intrinsic nature of biomolecules, including carbohydrates. For example, the studies of D-glucose and D-galactose were carried out using high-resolution Fourier transform microwave spectroscopy (FTMW) in conjunction with laser vaporization methods conducted in supersonic expansions.[22,23] Interestingly, the study of the C_1 epimerization effect in D-glucose shows that there are four stable conformers for α-D-glucopyranose and three for β-D-glucopyranose, with the most stable conformers stabilized by stereoelectronic hyperconjugative forces due to the gauche effect.[22] For α-D-galactose, the results show how the epimerization at C_4 drastically changes the conformational behaviour.[21] Therefore, the same methodology should work for studying the C_3 epimerization effect in glucose and allose. With this goal in mind, in this work, we chose to study the conformational behaviour of D-allose and compare the results with those previously obtained for D-glucose. It could allow us to answer several key questions: what should the effect of epimerization on the conformational behaviour of β-D-glucose and β-D-allose be? How does it affect the formation of the intramolecular hydrogen bonding networks? Do the intramolecular forces have any influence on their natural abundances? To answer these questions, in the following we present a rotational spectroscopic study of β-D-allose. As we will show, despite the main conformers of β-D-glucose and β-D-allose are very similar, the position of the hydroxyl groups in allose allows for the formation of considerably stronger intramolecular hydrogen bonds than in glucose. This could be the key to explain the low and high abundances of beta-D-allose and β-D-glucose in nature, respectively.

As shown in Figure 2, allose can adopt different configurations depending on the orientation of the hydroxymethyl group. A total of 33 stable structures of β-D-allose were obtained using the computational approach discussed in the Supplementary Information (SI). All the structures and relevant parameters are collected in Figure S2 and Tables S1-S2 of the Supporting Information. Among them, eight structures are below 1000 cm^{-1} relative to the global minimum. The eight most stable structures have a $^4C_1$ ring configuration, which confers them higher stability.

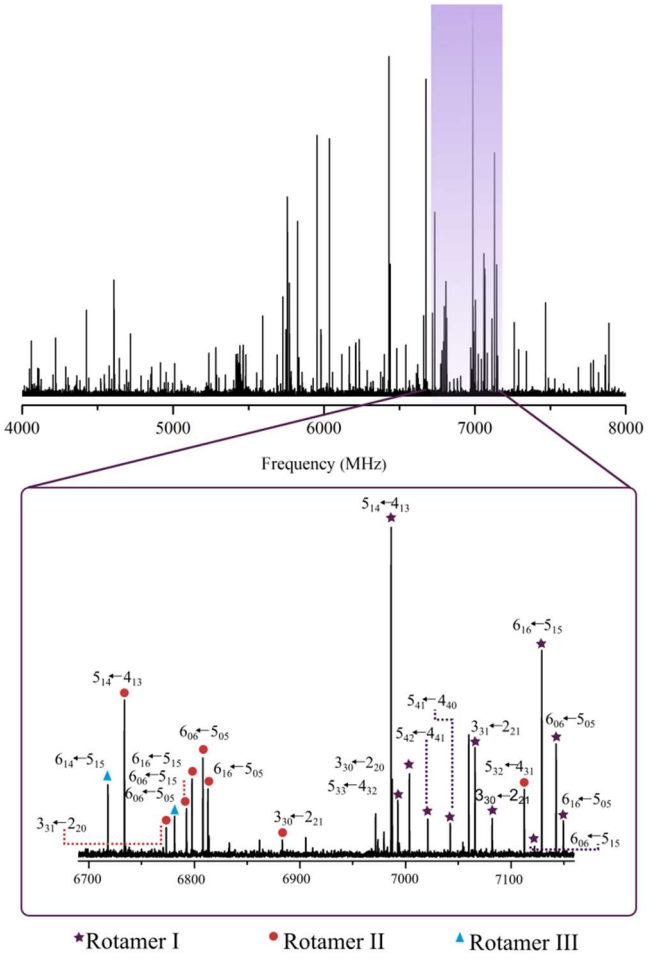

Fig. 3 Broadband CP-FTMW rotational spectrum of β-D-allose in the 4–8 GHz frequency region. Bottom: inset of the CP-FTMW spectrum showing selected rotational transitions ascribed to the three detected rotamers.

Interestingly, the six most stable conformers have a counterclockwise intramolecular hydrogen bond network between the hydroxyl groups, while the clockwise arrangement is energetically less stable. Among the six most stable structures, the structures differ in the orientation of the hydroxymethyl group, with those positioned towards the molecule (structures G-g+/cc/t, G+g-/cc/t, and Tg+/cc/t), being 800 cm^{-1} more stable than those with the hydroxymethyl group pointing outwards due to the extra hydrogen bond. Only the three most stable structures are expected to be populated enough in a supersonic expansion.[20,24–26]

In a second step, we used two LA-CP-FTMW spectrometers[21,27,28] to obtain the microwave spectrum of β-D-allose in the 4–14 GHz frequency range (details of the experimental procedure are given in the SI). As can be seen in Figure 3, the broadband rotational spectrum consists of several rotational lines, suggesting the presence of several conformers. We first removed the spectral signatures of known photofragmentation products[29] and turned our attention to the calculated spectroscopic parameters of the most energetically-stable conformers. All the low-lying conformers are prolate asymmetric tops with relatively high

Table 1. Experimental and calculated spectroscopic parameters for β-D-allose.

	Experimental			Theory / MP2/6-311++G(d,p)		
	I	II	III	G-g+/cc/t	G+g-/cc/t	Tg+/cc/t
A[a]	1267.54158(31)[g]	1230.06990(42)	1457.052(17)	1273.5	1232.9	1466.4
B	810.31204(19)	796.28806(22)	721.77324(78)	813.3	801.0	723.4
C	559.37787(22)	530.88028(14)	526.66014(67)	562.0	533.8	529.6
Δ_J	0.0150(12)	-	-	-	-	-
$\lvert\mu_a\rvert$	Observed	Observed	Observed	3.0	2.8	3.3
$\lvert\mu_b\rvert$	Observed	Observed	Not observed	1.6	1.5	0.2
$\lvert\mu_c\rvert$	Observed	Not observed	Not observed	2.2	0.4	0.4
σ[b]	10.8	16.8	15.1	-	-	-
N[c]	141	77	24	-	-	-
ΔE[d]	-	-	-	0	103	243
ΔE_{ZPE}[e]	-	-	-	0	76	290
ΔG[f]	-	-	-	0	45	320

[a]*A*, *B*, and *C* represent the rotational constants (in MHz); Δ_J is the quartic centrifugal distortion constant (in kHz); μ_a, μ_b, and μ_c are the electric dipole moment components (in D); [b]RMS deviation of the fit (in kHz). [c]Number of measured transitions. [d]Relative energies (in cm^{-1}) calculated at MP2 level respect to the global minimum. [e]Relative energies (in cm^{-1}) calculated at MP2 respect to the global minimum, taking into account the zero-point energy (ZPE). [f]Gibbs energies (in cm^{-1}) calculated at MP2 and 298 K. [g]Standard error in parentheses in units of the last digit.

values of the electric dipole moment component μ_a (see Table S1). For this reason, our conformational search focused on locating the set of characteristic *a*-type *R*-branch transitions, which are separated approximately *B*+*C*. The assignment of the first rotamer, rotamer I, was straightforward due to the intense *a*-type R-branch transitions that were fitted using a rigid rotor Hamiltonian.[30–32] The generated rotational constants allowed us to expand the assignments to the *b*- and *c*-type transitions. A total of 141 transitions were finally assigned: 65 *a*-type, 29 *b*-type, and 25 *c*-type *R*-branch transitions; other 22 *Q*-branch transitions were also included. The resulting rotational constants of rotamer I are collected in Table 1, while the list of the measured frequencies can be found in Table S3 of the supporting information.

After assigning all the rotational lines belonging to the first rotamer, we looked for other candidates. Another two rotamers were identified using the same procedure described above for rotamer I. 77 transitions, including *a*- and *b*-types, were measured for rotamer II, while only 24 *a*-type rotational transitions were observed for rotamer III. The transitions measured for rotamers II and III are contained in Tables S4 and S5, respectively. In addition, the experimentally obtained spectroscopic parameters for each species are listed in Table 1.

The assignment of each rotamer is straightforward. As can be seen in Table 1, there is a good correspondence between the experimental rotational constants of rotamer I with those calculated for the G-g+/cc/t structure. The selection rules further confirm the assignment as the dipole moment in the three axes have a significant value, and all types of rotational transitions were observed. Similarly, the experimental rotational constants and selection rules of rotamer II are in good agreement with those of the G+g-/cc/t structure. Finally, the rotational constants of rotamer III, which are radically different from the other two rotamers, along with the observance of only *c*-type transitions, are in good agreement with the predicted values of the Tg+/cc/t structure. We note how the calculated rotational constants agree very well with the experimental values. We calculated the scale factors by dividing the experimental rotational constants by the calculated ones. Scale factors ranging from 1.002 to 1.006 brings the predicted values of the rotational constants into coincidence with the experimental ones.[33,34]

We also estimated the relative population of the detected conformers based on the intensities of the rotational transitions and the predicted dipole moments. We found that the G-g+/cc/t and G+g-/cc/t structures have a similar abundance (50% and 40%, respectively), while the Tg+/cc/t structure is only about a 10%. These results are in good agreement with the estimated abundances using the relative energies.

Once the conformers have been identified, the main intramolecular interactions can be analyzed. The structures of the three experimental conformers of β-D-allose are shown in Figure 4 (Tables S6 to S8 collect their cartesian coordinates). As previously stated, the three conformers of β-D-allose anomer present a $^4C_1$ arrangement due to the presence of intramolecular interactions between the OH groups, which behave as bifunctional entities, acting as proton donors or proton acceptors. This cooperative hydrogen bonding network observed for all shapers is arranged counterclockwise and is made up of the series O_4H (eq) → O_3H (ax) → O_2H (eq) → O_1H (eq). The three detected conformers, which are also the three most stable structures, only differ in the orientation of the CH_2OH group.

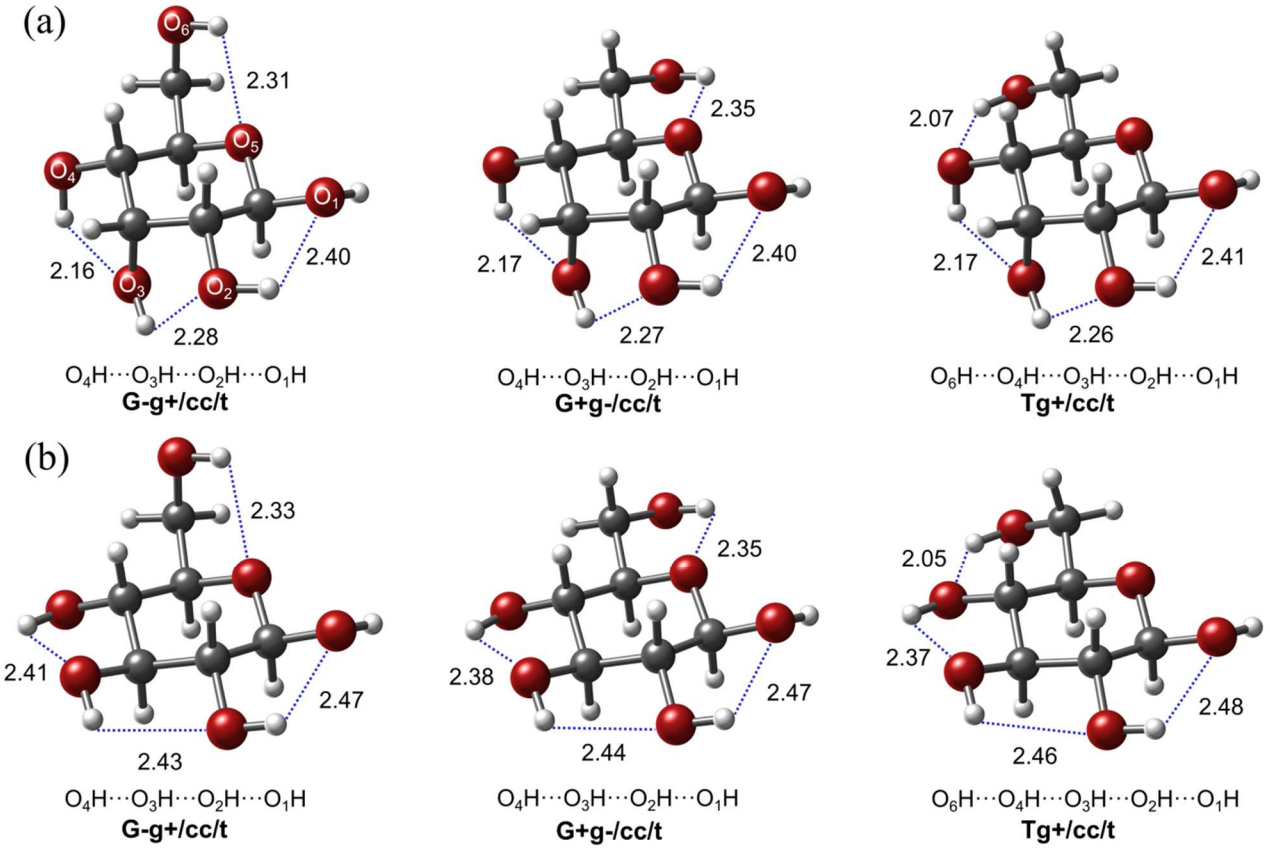

Fig. 4 (a) Three-dimensional structures of the three observed conformers of β-D-allose showing the cooperative intramolecular hydrogen-bonding networks. (b) A comparison with the observed structures of β-D-glucose[22]. The distances are given in Å.

Once the conformers have been identified, the main intramolecular interactions can be analyzed. The structures of the three experimental conformers of β-D-allose are shown in Figure 4 (Tables S6 to S8 collect their cartesian coordinates). As previously stated, the three conformers of β-D-allose anomer present a $^4C_1$ arrangement due to the presence of intramolecular interactions between the OH groups, which behave as bifunctional entities, acting as proton donors or proton acceptors. This cooperative hydrogen bonding network observed for all shapers is arranged counterclockwise and is made up of the series O_4H (eq) → O_3H (ax) → O_2H (eq) → O_1H (eq). The three detected conformers, which are also the three most stable structures, only differ in the orientation of the CH_2OH group.

We now proceed to analyze the effect of epimerization. As previously stated, both the C_1 and C_4 epimerizations have some notorious changes: for the C_1 epimerization an extra conformer is observed in α-D-glucopyranose,[22] while for the C_4 epimerization it drastically changes the conformational behaviour by altering the abundances of the most stable conformers, as well as the main intramolecular forces that stabilizes them.[21] Figure 4 compares the intramolecular hydrogen bond distances for the detected conformers of β-D-allose and β-D-glucose. Interestingly, the comparison, a priori, seems to indicate that both structures behave similarly: for both molecules, three stable conformers have been detected. They all present a cooperative intramolecular network involving the O_4H (eq) → O_3H (eq) → O_2H (eq) → O_1H (eq) functional groups, and the relative population of the two most stable structures is about 45% each, while the third conformer is a minor species (about 10% of the relative population). Thus, a first impression is that epimerization at C_3 does not have any significant influence. There are, however, some important differences between both epimers. The conformers of β-D-glucose exhibit weaker intramolecular hydrogen bonds than those of β-D-allose. This is due to all hydroxyl groups being in an equatorial arrangement and therefore in alternate positions, enlarging the non-covalent bond distances,[22,23,35] the O_4H (eq) → O_3H (eq) → O_2H (eq) hydrogen bond distances decrease about 0.2 Å when going from β-D-glucose to β-D-allose. In order to evaluate the strength of the intramolecular hydrogen bonds within each sugar, we carried out a computerized numerical analysis and graphic user-assisted interpretation of the electronic density (ρ) and its derivatives using the NCIplot program.[36,37] The results are collected in Figure 5. There is indeed a relatively strong cooperative hydrogen bond network for β-D-allose in contrast to β-D-glucose, which shows very weak non-covalent interactions for the O_4H→O_3H and O_3H→O_2H intramolecular interactions.

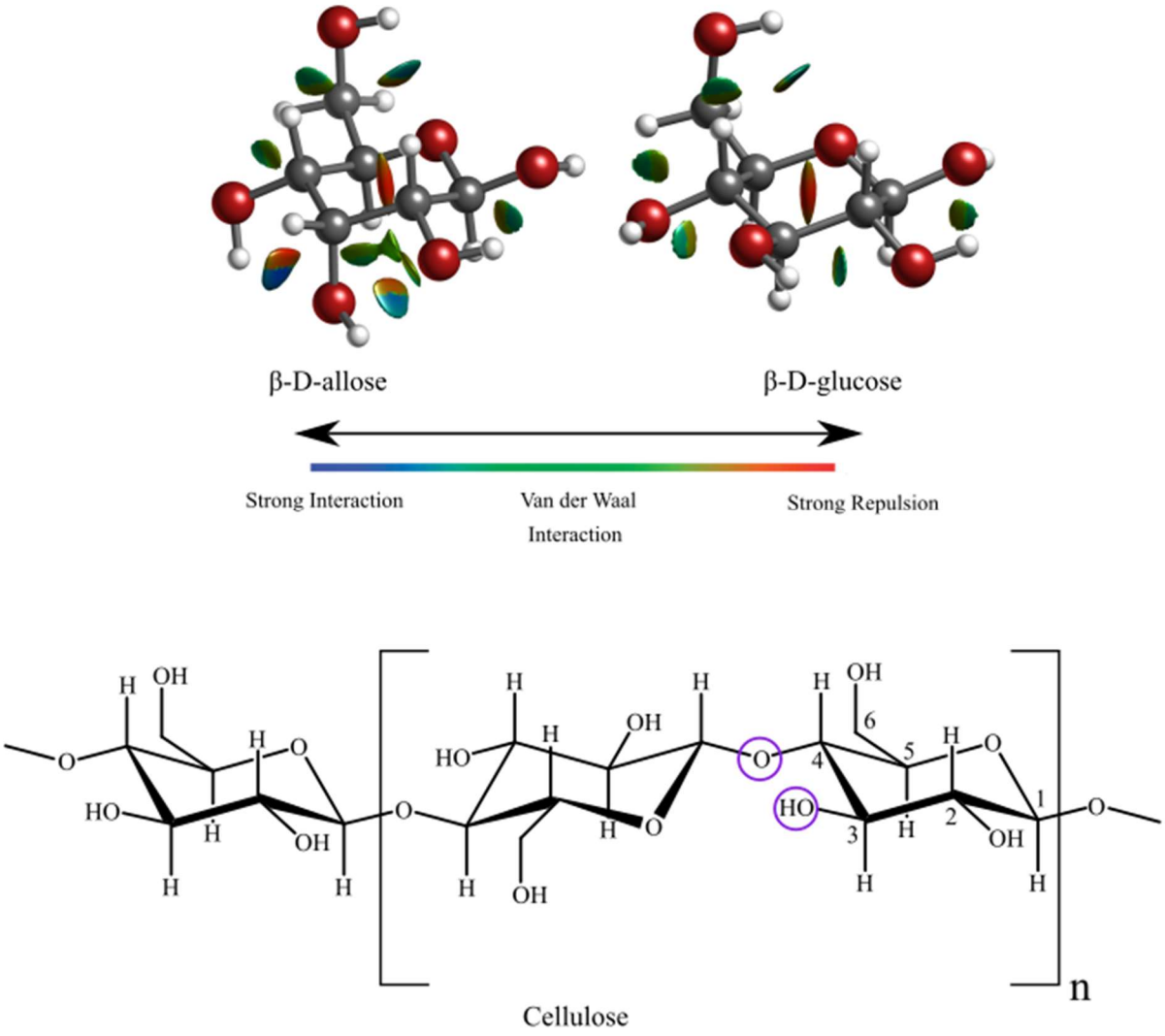

Fig. 5 Top: the non-covalent interactions of the most stable conformer (G-g+/cc/t) of β-D-allose and β-D-glucose. Bottom: the unbranched polymer of β-D-glucose occurs through the linkage of β(1→4) D-glucose units. The responsible hydroxyl functional groups (O_3H and O_4H) that have a strong intramolecular hydrogen bond in β-D-allose but weaker in β-D-glucose are encircled.

One exciting outcome of the differences in the intermolecular interactions of allose and glucose is related to their biological function. As explained earlier, cellulose is an unbranched polymer of β-D-glucose, and it is among the most abundant organic compounds in the biosphere, while β-D-allose barely exists in nature. But why has evolution selected the former as the most abundant organic polymer on Earth? One possible interpretation could be that it is due to their differences in the strength of the intramolecular interactions discussed above: the cellulose polysaccharide requires the construction of a linear chain of several hundred to many thousands of β(1→4) linked D-glucose units (see Figure 5); because this covalent bond happens through the O_4H hydroxyl group of the anomeric C_4 carbon, the formation of such polysaccharides should be statistically more favorable if the O_4H is easier to attack. In β-D-glucose, the hydrogen bond is considerably weaker than in β-D-allose, and thus the energetic cost to polymerize the former should be considerably lower as it requires breaking a weaker bond.

In summary, the combination between laser ablation and rotational spectroscopy has allowed us to identify the conformational preferences of the β-D-Allose carbohydrate unequivocally. Three conformers have been identified and show a cooperative network of hydrogen bonds (O_4H (eq) → O_3H (ax) → O_2H (eq) → O_1H (eq)) in a counterclockwise (cc) arrangement. The three conformers only differ in the orientation of the hydroxymethyl group. The effect of epimerization on the C_3 atom has also been investigated by comparing the results of β-D-allose and β-D-glucose. Despite the main conformers being very similar, the cooperative hydrogen bond network in allose is considerably stronger than that in glucose. This could be the reason why cellulose, an unbranched polymer of β-D-glucose, is among the most abundant organic compounds in the biosphere, while β-D-allose is scarce.

Conflicts of interest

There are no conflicts to declare.

Acknowledgments

The financial fundings from Ministerio de Ciencia e Innovación (PID2019-111396GB-I00), Junta de Castilla y León (VA244P20) and European Research Council under the European Union's Seventh Framework Programme (FP/2007-2013) / ERC-2013-SyG, Grant Agreement n. 610256 NANOCOSMOS, are gratefully acknowledged. G.J. acknowledges funding from the Spanish "Ministerio de Ciencia, Innovación y Universidades" under predoctoral FPI Grant (BES-2017-082173).

Notes and references

1 A. Blanco and G. Blanco, *Medical Biochemistry*, Academic Press, United Kingdom, 2017.

2 K. G. Ramawat and J. M. Mérillon, *Polysaccharides: Bioactivity and biotechnology*, Springer International Publishing, 2015.

3 S. P. Bhutani, *Chemistry of Biomolecules, Second Edition*, Taylor & Francis Ltd, 2019.

4 K. Izumori, Izumoring: A strategy for bioproduction of all hexoses, *J. Biotechnol.*, 2006, **124**, 717–722.

5 R. U. Lemieux, *Explorations with Sugars: How Sweet It Was*, Washington, DC, American C., 1990.

6 P. M. Collins and R. J. Ferrier, *Monosaccharides : their chemistry and their roles in natural products*, Wiley & Sons, New York, 1995.

7 F. Yamaguchi, M. Takata, K. Kamitori, M. Nonaka, Y. Dong, L. Sui and M. Tokuda, Rare sugar D-allose induces specific up-regulation of TXNIP and subsequent G1 cell cycle arrest in hepatocellular carcinoma cells by stabilization of p27kip1, *Int. J. Oncol.*, 2008, **32**, 377–385.

8 B. P. Beylis and G. W. Perold, The Occurrence of D- (+) - Allose in Nature, 1971, **11**, 1971.

9 A. D. Mooradian, M. Smith and M. Tokuda, The role of artificial and natural sweeteners in reducing the consumption of table sugar: A narrative review, *Clin. Nutr. ESPEN*, 2017, **18**, 1–8.

10 Y. Iga, K. Nakamichi, Y. Shirai and T. Matsuo, Acute and Sub-Chronic Toxicity of D -Allose in Rats, *Biosci. Biotechnol. Biochem.*, 2010, **74**, 1476–1478.

11 S. P. Bhutani, *Chemistry of Biomolecules*, 2019.

12 L. M. J. Kroon-Batenburg, P. Van der Sluis and J. A. Kanters, Structure of β-D-Allose, C6H12O6, *Acta Cryst.*, 1984, **2**, 1863–1865.

13 A. J. Ragauskas, C. K. Williams, B. H. Davison, G. Britovsek, J. Cairney, C. A. Eckert, W. J. Frederick, J. P. Hallett, D. J. Leak, C. L. Liotta, J. R. Mielenz, R. Murphy, R. Templer and T. Tschaplinski, The path forward for biofuels and biomaterials, *Science (80-.).*, 2006, **311**, 484–489.

14 J. L. Alonso and J. C. López, in *Topics in Current Chemistry*, eds. A. M. Rijs and J. Oomens, SpringerLink, 2015, vol. 364, pp. 335–402.

15 P. Hobley, O. Howarth and R. N. Ibbett, 1H and 13C NMR shifts for aldopyranose and aldofuranose monosaccharides: Conformational analysis and solvent dependence, *Magn. Reson. Chem.*, 1996, **34**, 755–760.

16 S. J. Angyal, The Composition and Conformation of Sugars in Solution, *Angew. Chemie Int. Ed. English*, 1969, **8**, 157–166.

17 P. K. Bose and P. L. Polavarapu, Vibrational circular dichroism of monosaccharides, *Carbohydr. Res.*, 1999, **319**, 172–183.

18 L. D. Barron, Z. Q. Wen and L. Hecht, Vibrational Raman Optical Activity of Proteins, *J. Am. Chem. Soc.*, 1992, **114**, 784–786.

19 G. G. Brown, B. C. Dian, K. O. Douglass, S. M. Geyer and B. H. Pate, The rotational spectrum of epifluorohydrin measured by chirped-pulse Fourier transform microwave spectroscopy, *J. Mol. Spectrosc.*, 2006, **238**, 200–212.

20 C. Cabezas, M. Varela and J. L. Alonso, The Structure of the Elusive Simplest Dipeptide Gly-Gly, *Angew. Chemie Int. Ed.*, 2017, **129**, 6520–6525.

21 E. R. Alonso, I. León and J. L. Alonso, in *Intra- and Intermolecular Interactions Between Non-covalently Bonded Species*, Elsevier, 2021, pp. 93–141.

22 J. L. Alonso, M. A. Lozoya, I. Peña, J. C. López, C. Cabezas, S. Mata and S. Blanco, The conformational behaviour of free d -glucose—at last, *Chem. Sci.*, 2014, **5**, 515–522.

23 I. Peña, C. Cabezas and J. L. Alonso, Unveiling epimerization effects: a rotational study of alpha-D-galactose., *Chem. Commun. (Camb).*, 2015, **51**, 10115–10118.

24 R. S. Ruoff, T. D. Klots, T. Emilsson and H. S. Gutowsky, Relaxation of conformers and isomers in seeded supersonic jets of inert gases, *J. Chem. Phys.*, 1990, **93**, 3142–3150.

25 P. D. Godfrey, R. D. Brown and F. M. Rodgers, The missing conformers of glycine and alanine: relaxation in seeded supersonic jets, *J. Mol. Struct.*, 1996, **376**, 65–81.

26 I. León, E. R. Alonso, S. Mata and J. L. Alonso, A rotational study of the AlaAla dipeptide, *Phys. Chem. Chem. Phys.*, 2020, **22**, 13867–13871.

27 I. León, E. R. Alonso, S. Mata and J. L. Alonso, Shape of Testosterone, *J. Phys. Chem. Lett.*, 2021, **12**, 6983–6987.

28 M. Sanz-Novo, M. Mato, I. León, A. M. Echavarren and J. L. Alonso, Shape-Shifting Molecules: Unveiling the Valence Tautomerism Phenomena in Bare Barbaralones, *Angew. Chemie - Int. Ed.*, 2022, **61**, 1–6.

29 L. Kolesniková, I. León, E. R. Alonso, S. Mata and J. L. Alonso, Laser Ablation Assists Cyclization Reactions of Hydantoic Acid: A Proof for the Near-Attack Conformation Theory?, *J. Phys. Chem. Lett.*, 2019, **10**, 1325–1330.

30 D. F. Plusquellic, JB95 Spectral fitting program | NIST, https://www.nist.gov/services-resources/software/jb95-spectral-fitting-program.

31 W. Gordy and R. L. Cook, *Microwave Molecular Spectroscopy*, New York, 1984.

32 H. M. Pickett, The fitting and prediction of vibration-rotation spectra with spin interactions, *J. Mol. Spectrosc.*,

1991, **148**, 371–377.

33 M. Sanz-Novo, E. R. Alonso, I. León and J. L. Alonso, The Shape of the Archetypical Oxocarbon Squaric Acid and Its Water Clusters, *Chem. - A Eur. J.*, 2019, **25**, 10748–10755.

34 G. Juárez, M. Sanz-Novo, J. L. Alonso, E. R. Alonso and I. León, Rotational Spectrum and Conformational Analysis of Perillartine: Insights into the Structure–Sweetness Relationship, *Molecules*, 2022, **27**, 1924.

35 I. Peña, S. Mata, A. Martín, C. Cabezas, A. M. Daly and J. L. Alonso, Conformations of D-xylose: the pivotal role of the intramolecular hydrogen-bonding., *Phys. Chem. Chem. Phys.*, 2013, **15**, 18243–8.

36 R. Chaudret, B. De Courcy, J. Contreras-García, E. Gloaguen, A. Zehnacker-Rentien, M. Mons and J. P. Piquemal, Unraveling non-covalent interactions within flexible biomolecules: From electron density topology to gas phase spectroscopy, *Phys. Chem. Chem. Phys.*, 2014, **16**, 9876–9891.

37 J. Contreras-García, E. Gloaguen, R. Chaudret, M. Mons, A. Zehnacker-Rentien, B. de Courcy and J.-P. Piquemal, Unraveling non-covalent interactions within flexible biomolecules: from electron density topology to gas phase spectroscopy, *Phys. Chem. Chem. Phys.*, 2013, **16**, 9876.